

Evolution of Light-Like Wilson Loops with a Self-Intersection in Loop Space

T. Mertens* and P. Taels†

*Departement Fysica, Universiteit Antwerpen,
B-2020 Antwerpen, Belgium*

(Dated: October 26, 2018)

Abstract

Recently, we proposed a general evolution equation for single quadrilateral Wilson loops on the light-cone. In the present work, we study the energy evolution of a combination of two such loops that partially overlap or have a self-intersection. We show that, for a class of geometric variations, then evolution is consistent with our previous conjecture, and we are able to handle the intricacies associated with the self-intersections and overlaps. This way, a step forward is made towards the understanding of loop space, with the hope of studying more complicated structures appearing in phenomenological relevant objects, such as parton distributions.

PACS numbers: 12.38.-T, 03.70.+K, 11.10.-Z

arXiv:1308.5296v2 [hep-ph] 3 Sep 2013

*Electronic address: tom.mertens@uantwerpen.be

†Electronic address: pieter.taels@uantwerpen.be

1. INTRODUCTION

A reformulation of the Ambrose-Singer theorem in a gauge theory context [1] states that the holonomy variables U_Γ of the (gauge-)connection $\mathcal{A}_\mu = A_\mu^a t^a$:

$$U_{\Gamma_i} = \Phi(\Gamma_i) = \mathcal{P} \exp \left[ig \oint_{\Gamma_i} dz^\mu \mathcal{A}_\mu(z) \right], \quad (1)$$

where the Γ_i are loops, and where t^a are the generators of the Lie algebra of the gauge group in a certain representation (here the fundamental representation of $SU(N_c)$), contain the same information as the corresponding gauge theory. From this holonomy, which is some $N \times N$ matrix in the representation of the gauge group, a gauge invariant variable can be obtained by taking the trace¹. This trace introduces, however, extra constraints on the loops: the so-called Mandelstam constraints [1–4], which assure that the product of traces over holonomies is again the trace of a holonomy. Gauge theory can then be represented in a loop space setting, where the observables are now built from the vacuum expectation values of products of traces of holonomies, referred to as Wilson loop variables [2, 3, 5–7]:

$$\mathcal{W}_n[\Gamma_1, \dots, \Gamma_n] = \left\langle 0 \left| \mathcal{T} \frac{1}{N_c} \text{Tr} \Phi(\Gamma_1) \cdots \frac{1}{N_c} \text{Tr} \Phi(\Gamma_n) \right| 0 \right\rangle. \quad (2)$$

In a previous paper [8], we calculated the leading order contribution of a quadrilateral Wilson loop on the light-cone, and introduced a new differential operator:

$$\frac{d}{d \ln \sigma} = s \frac{d}{ds} + t \frac{d}{dt}, \quad (3)$$

with s and t the Mandelstam variables (see section 2). This operator was then used to derive an evolution equation for this class of Wilson loops, and inspired us to formulate a conjecture for a general evolution equation:

$$\lim_{\epsilon \rightarrow 0} \mu \frac{d}{d\mu} \left(\frac{d}{d \ln \sigma} \mathcal{W}_1(\Gamma) \right) = - \sum_{cusps} \Gamma_{cusp}, \quad (4)$$

where ϵ is defined in the dimensional regularization procedure $D = 4 - 2\epsilon$. It was also shown that the evolution of the cusp and Π -shape configurations is consistent with this conjecture (see [8] for the details). It turns out that the operator, Eq. (4), is a special case of the Fréchet derivative [9, 10], the details of which will be discussed elsewhere [11].

In this work, we consider some symmetrical combinations of two quadrilateral Wilson loops on the light-cone, for which we test conjecture (4). Put in a Wilson loop variable language: we are calculating $\mathcal{W}_1[\Gamma]$, with $\Gamma = \Gamma_1 \Gamma_2$, where the product between the loops is defined in generalized loop space [12]. Important is that these Wilson loop configurations exhibit intricacies, associated with the self-intersection and overlap, that usually cause problems in a loop space approach. A close inspection of these intricacies indicate that one needs to be careful in counting cusps along the path. We show that the effective number of cusps can deviate from the number one would expect from a naive counting procedure. Furthermore, the group structure of loop space is confirmed by our explicit calculations.

¹ U_Γ transforms under a gauge transformation as $U_\Gamma^g = g_x^{-1} U_\Gamma g_x$, where $x = \Gamma(0)$. The cyclicity of the trace assures that $\text{Tr} U_\Gamma$ is gauge invariant.

2. LOOPS AND PARAMETRIZATION

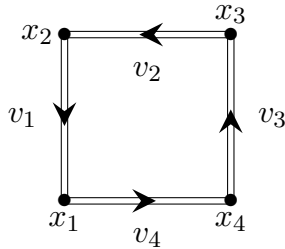


Figure 1: Parametrization of the Wilson Loop in coordinate space.

We combine two similar quadrilateral Wilson loops on the light-cone in two different configurations: with a partial overlap (figures 2 to 3), and with a self-intersection (figures 4 to 5). Each loop is parametrized by four vectors v_i on the light-cone (i.e. $v_i^2 = 0, \forall i$), as shown in figure 1. In the symmetric cases under consideration, both loops are equal in size and hence can be parametrized by these four vectors. We also introduce the Mandelstam variables²

$$s = (v_1 + v_2)^2 = 2v_1v_2, \quad t = (v_2 + v_3)^2 = 2v_2v_3, \quad (5)$$

in order to simplify the notation of the results of the calculation. Each configuration has two different possible relative orientations for the constituting loops: one where the orientation is equal (figures 2 and 5) and one where the orientation is opposite (figures 3 and 4). These orientations define how the Wilson line - gluon vertices are ordered along the path, and also fix the color flow at the self-intersection or overlap. In the figures, the color flow along the loops is represented by the different arrow styles, and the point \mathbf{x}_1 represents the base-point of the considered loop space. Here we only consider color neutral objects, in other words: there are no gluons in the initial or final state.

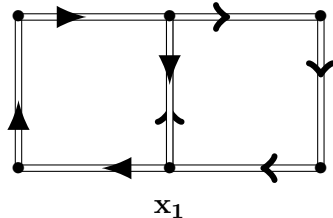


Figure 2: Configuration 1

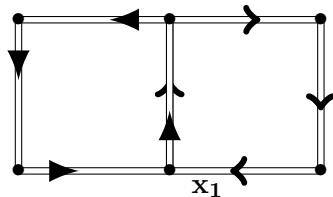


Figure 3: Configuration 2

² Note the signs!

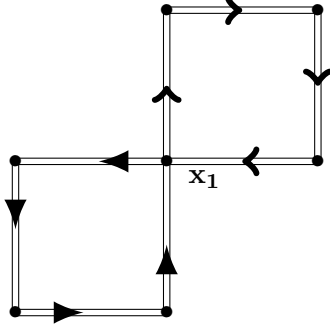


Figure 4: Configuration 3

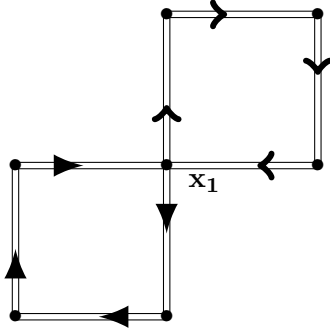


Figure 5: Configuration 4

3. LOOP-GROUP STRUCTURE

Expanding Eq. (1) to second order

$$\Phi(\Gamma) = 1 + ig \oint_{\Gamma} dz^{\mu} \mathcal{A}_{\mu}(z) - \frac{g^2}{2!} \mathcal{P} \oint_{\Gamma} dz^{\mu} dz^{\nu} \mathcal{A}_{\mu}(z) \mathcal{A}_{\nu}(z'), \quad (6)$$

and taking traces and vacuum expectation values yields:

$$\mathcal{W}_1(\Gamma) = 1 - \frac{g^2}{2!} \text{Tr}(t^a t^b) \langle 0 | \mathcal{T} \oint_{\Gamma} dz^{\mu} dz^{\nu} A_{\mu}^a(z) A_{\nu}^b(z') | 0 \rangle, \quad (7)$$

for the first order Wilson loop variable. The generators and gauge connections in Eq. (7) are ordered along the loop by the time-ordering operation \mathcal{T} , where the “time” is represented by the path parameter $t \in [0, 1]$ such that $dz^{\mu} = \dot{z}^{\mu} dt$. Now, considering $\Gamma = \Gamma_1 \Gamma_2$, the group structure of generalized loop space [12–15] allows us to rewrite the integral in the second term of Eq. (7) as

$$\oint_{\Gamma_1 \Gamma_2} \mathcal{A}_{\mu} \mathcal{A}_{\nu} = \oint_{\Gamma_1} \mathcal{A}_{\mu} \mathcal{A}_{\nu} + \oint_{\Gamma_1} \mathcal{A}_{\mu} \oint_{\Gamma_2} \mathcal{A}_{\nu} + \oint_{\Gamma_2} \mathcal{A}_{\mu} \mathcal{A}_{\nu}, \quad (8)$$

where \mathcal{A}_{μ} and \mathcal{A}_{ν} are again ordered along the path³ and the integral measures are suppressed. Eq. (8) makes it clear that there are three contributions: two coming from the loops considered independently, and one coming from the interference terms. Also, the group structure

³ This means we do not need to consider the contribution $\int_{\Gamma_1} \mathcal{A}_{\nu} \int_{\Gamma_2} \mathcal{A}_{\mu}$.

of generalized loop space⁴ takes care of what happens when one changes the orientation of one of the two loops :

$$\begin{aligned} \oint_{\Gamma_1\Gamma_2^{-1}} \mathcal{A}_\mu \mathcal{A}_\nu &= \int_{\Gamma_1} \mathcal{A}_\mu \mathcal{A}_\nu + \int_{\Gamma_1} \mathcal{A}_\mu \int_{\Gamma_2^{-1}} \mathcal{A}_\nu + \int_{\Gamma_2^{-1}} \mathcal{A}_\mu \mathcal{A}_\nu \\ &= \int_{\Gamma_1} \mathcal{A}_\mu \mathcal{A}_\nu + (-1)^1 \int_{\Gamma_1} \mathcal{A}_\mu \int_{\Gamma_2} \mathcal{A}_\nu + (-1)^2 \int_{\Gamma_2} \mathcal{A}_\nu \mathcal{A}_\mu . \end{aligned} \quad (9)$$

In the last term, the order of the algebra generators inside the trace needs to be reversed as well (i.e. $\text{Tr}(t^a t^b) \rightarrow \text{Tr}(t^b t^a)$). However, due to the cyclicity of the trace, at one-loop level both traces yield the same result. Moreover, in the first order, the value of the Wilson loop variables of the single loops: the first and last term in (8), are independent of the orientation of the loop. Therefore, we can immediately write down the single loop contributions to Eq. (9) from our previous results in [8] (see Eq. (11)).

4. DIAGRAM RESULTS

Using the dimensionally regularized gluon propagator in the Feynman gauge and in coordinate representation:

$$D_{\mu\nu}^{ab}(z - z') = \frac{(\mu^2\pi)^\epsilon}{4\pi^2} \Gamma[1 - \epsilon] g_{\mu\nu} \delta^{ab} \frac{1}{(-|z - z'|^2 - i0)^{1-\epsilon}}, \quad (10)$$

we obtain for a single quadrilateral loop on the light-cone [8, 16–18]:

$$\mathcal{W}_1(\Gamma_1) = \mathcal{W}_1(\Gamma_2) \approx 1 - \frac{N_c \alpha_s \pi^\epsilon}{2\pi} \Gamma[1 - \epsilon] \left(\frac{1}{\epsilon^2} (-s\mu^2)^\epsilon + \frac{1}{\epsilon^2} (-t\mu^2)^\epsilon - \frac{1}{2} \ln\left(\frac{s}{t}\right)^2 + \text{finite} \right) + \mathcal{O}(\alpha_s^2), \quad (11)$$

where we took the large N_c limit [3, 19–21] and assumed that Γ_1 and Γ_2 are equal in size. The interference terms of Eq. (7) are computed as follows: let us consider, for example, one of the diagrams that contribute to the interference term of configuration 4 (figure 5), which is shown in figure 6. In order to calculate this diagram, we parametrize the coordinates z

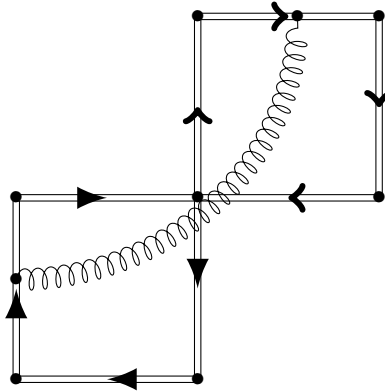


Figure 6: Configuration 4: example of an interference diagram

⁴ The group structure was confirmed by explicit calculation of the full diagrams.

and z' from the gluon propagator along the relevant parts of the path as follows:

$$z = x_1 - v_1 - xv_2, \quad x \in [0, 1] \quad z' = x_1 + v_2 + (1 - y)v_1, \quad y \in [0, 1], \quad (12)$$

so that the denominator of gluon propagator becomes:

$$(-(z - z')^2)^{1-\epsilon} = (-2v_1v_2(1+x)(2-y))^{1-\epsilon}. \quad (13)$$

The integral measure $dz dz'$ in this case becomes $v_1v_2 dx dy = \frac{s}{2}dx dy$, hence:

$$\begin{aligned} -\frac{C_F g^2}{N_c} \frac{1}{2} \int_{\Gamma_1} A_\mu(z) dz \int_{\Gamma_2} A_\nu(z') dz' &= -\frac{C_F g^2 (\mu^2 \pi)^\epsilon}{N_c} \frac{1}{4\pi^2} \Gamma[1-\epsilon] \frac{1}{2} \int_0^1 \int_0^1 dx dy \frac{(-s)}{(-s(1+x)(2-y))^{1-\epsilon}} \\ &\approx -\frac{N_c \alpha_s \pi^\epsilon}{2\pi} \Gamma[1-\epsilon] \frac{1}{2} (-s)^\epsilon \frac{1}{\epsilon^2} (2^\epsilon - 1)^2, \end{aligned} \quad (14)$$

in the large N_c limit. Similar calculations can be done for the other diagrams and configurations. After summing all the contributions, this results in the following expressions for the considered configurations in the large N_c limit (the index refers to the configuration number):

$$\left[\left\langle 0 \left| \oint_{\Gamma_1 \Gamma_2} A_\mu A_\nu \right| 0 \right\rangle \right]_1 \approx \frac{N_c \alpha_s (\pi \mu^2)^\epsilon}{2\pi} \Gamma[1-\epsilon] \frac{1}{\epsilon^2} \left((-s)^\epsilon + (-t)^\epsilon - (2^\epsilon - 1) [(-t)^\epsilon + (-s)^\epsilon] \right) + \text{finite} + \mathcal{O}(\epsilon) \quad (15)$$

$$\left[\left\langle 0 \left| \oint_{\Gamma_1 \Gamma_2^{-1}} A_\mu A_\nu \right| 0 \right\rangle \right]_2 \approx -\frac{N_c \alpha_s (\pi \mu^2)^\epsilon}{2\pi} \Gamma[1-\epsilon] \frac{1}{\epsilon^2} \left((-s)^\epsilon + (-t)^\epsilon - (2^\epsilon - 1) [(-t)^\epsilon + (-s)^\epsilon] \right) + \text{finite} + \mathcal{O}(\epsilon) \quad (16)$$

$$\left[\left\langle 0 \left| \oint_{\Gamma_1 \Gamma_2^{-1}} A_\mu A_\nu \right| 0 \right\rangle \right]_3 \approx \frac{N_c \alpha_s (\pi \mu^2)^\epsilon}{2\pi} \Gamma[1-\epsilon] \frac{1}{\epsilon^2} \left((-s)^\epsilon - 2(-s)^\epsilon (2^\epsilon - 1) + (-s)^\epsilon (2^\epsilon - 1)^2 \right) + \text{finite} + \mathcal{O}(\epsilon) \quad (17)$$

$$\left[\left\langle 0 \left| \oint_{\Gamma_1 \Gamma_2} A_\mu A_\nu \right| 0 \right\rangle \right]_4 \approx -\frac{N_c \alpha_s (\pi \mu^2)^\epsilon}{2\pi} \Gamma[1-\epsilon] \frac{1}{\epsilon^2} \left((-s)^\epsilon - 2(-s)^\epsilon (2^\epsilon - 1) + (-s)^\epsilon (2^\epsilon - 1)^2 \right) + \text{finite} + \mathcal{O}(\epsilon), \quad (18)$$

It should be clear from Eq. (9) that, at one-loop order, the sign of the interference term changes when reversing the orientation of one of the loops, which is indeed confirmed by Eqs. (15) to (18).

5. DIFFERENTIAL OPERATOR

Finally, we want to apply the differential operator (3) followed by the operator $\mu \frac{d}{d\mu}$, to the considered loop configurations, after which we take the $\epsilon \rightarrow 0$ limit. Only symmetric variations⁵⁶ are taken into account, in such a way that the complete loop does not changes

⁵ Due to the fact that $s \frac{d}{ds} = (2s) \frac{d}{d(2s)}$ and $t \frac{d}{dt} = (2t) \frac{d}{d(2t)}$ we only need to consider $s \frac{d}{ds} + t \frac{d}{dt}$

⁶ Non-symmetric variations are now being studied by us, the results will be reported separately [22].

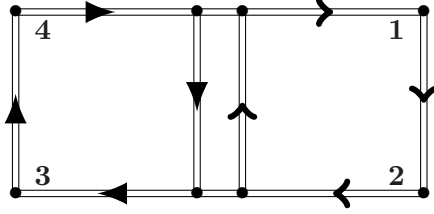


Figure 7: Configuration 1 reduced cusps (with overlapping paths separated)

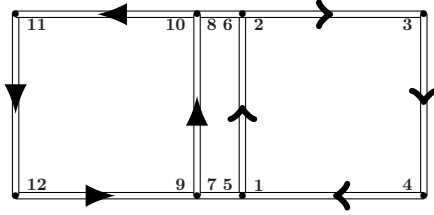


Figure 8: Configuration 2 extra cusps (with overlapping paths separated)

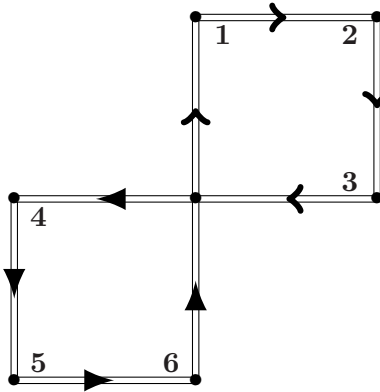


Figure 9: Configuration 3 reduced number of cusps

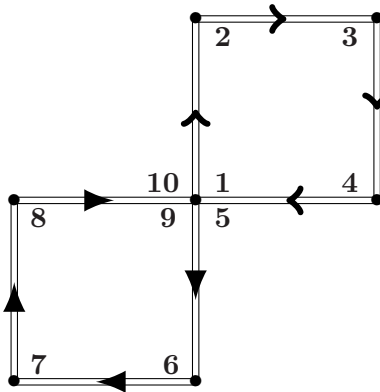


Figure 10: Configuration 4 extra cusps

its general structure. Indeed, if one does consider structure changing variations, the number

of cusps change and in [23]⁷ we will show explicitly that there is no continuous deformation in loop space between two structurally different loops (i.e. loops with a different number of cusps). The variations we apply here are shown in figures 11 to 14. Applying the said combination of operators to the different configurations in the $\epsilon \rightarrow 0$ and large N_c limits yields the following results:

$$\lim_{\epsilon \rightarrow 0} \mu \frac{d}{d\mu} \frac{d \ln (\mathcal{W}_1(\Gamma))_1}{d \ln \sigma} = -4\Gamma_{cusp} \quad (19)$$

$$\lim_{\epsilon \rightarrow 0} \mu \frac{d}{d\mu} \frac{d \ln (\mathcal{W}_1(\Gamma))_2}{d \ln \sigma} = -12\Gamma_{cusp} \quad (20)$$

$$\lim_{\epsilon \rightarrow 0} \mu \frac{d}{d\mu} \frac{d \ln (\mathcal{W}_1(\Gamma))_3}{d \ln \sigma} = -6\Gamma_{cusp} \quad (21)$$

$$\lim_{\epsilon \rightarrow 0} \mu \frac{d}{d\mu} \frac{d \ln (\mathcal{W}_1(\Gamma))_4}{d \ln \sigma} = -10\Gamma_{cusp}, \quad (22)$$

where

$$\Gamma_{cusp} \approx \frac{\alpha_s N_c}{2\pi} + \mathcal{O}(\alpha_s^2). \quad (23)$$

Naively counting the number of cusps in the different configurations yields a total of eight, in each configuration. If this is true, however, the results contradict our conjecture Eq. (4) [8]: indeed, we would expect for all the configurations a value of $-8\Gamma_{cusp}$ in the r.h.s. To understand this apparent contradiction, one has to take a closer look at how to count the number of cusps effectively present in the studied loop. Due to path reduction [12–15], configuration 1 (figure 2)⁸ can be reduced to a single quadrilateral so that there are effectively only four cusps (see also figure 7). Figure 8 shows how count the number of cusps in configuration 2 (figure 3). Here the extra cusps stem from the fact that the middle line is crossed twice in the same direction by the color flow along the path, so that these four cusps⁹ contribute twice to the total number of cusps. Similar reasoning can be applied to configurations 3 (figure 4) and 4 (figure 5), where the counting is demonstrated in figures 9 and 10 respectively.

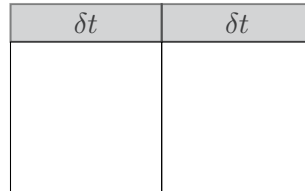


Figure 11: δt variation of the first two configurations

⁷ In preparation for publication.

⁸ We separated the overlapping paths in the figure to clarify the counting procedure.

⁹ Four because the cusps left and right of the middle path show up in the calculations of the interference contribution.

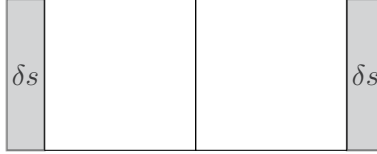


Figure 12: δs variation of the first two configurations

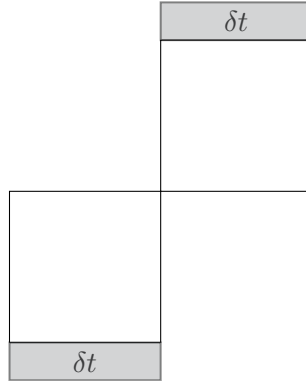


Figure 13: δt variation of the second two configurations

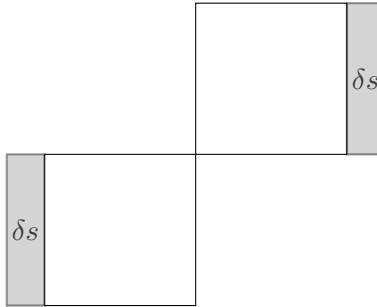


Figure 14: δs variation of the second two configurations

6. CONCLUSIONS AND REMARKS

By explicit calculation, we have showed that the symmetric double Wilson loops obey the generalized loop space group structure with respect to the inverse and the product of two loops. We also showed that the presented results are consistent with our evolution conjecture in [8]. At the same time, we successfully dealt with some of the intricacies, caused by a self intersection and a partial overlap, that appear in calculations of Wilson loops as functionals in loop space. This opens the door to the calculation of more complicated structures, such as the ones appearing in the calculations of transverse dependent momentum distributions (TMDs) or soft factors in certain factorization schemes in QCD [24, 25].

We would also like to point out that, when considering planar Wilson loops on the light-cone, the number of cusps seem to behave like a winding number of some sort, in the sense that in some cases the cusps add, and in other cases they subtract. Also note that from a loop space point of view, loops on the light-cone with a different number of cusps can not be

deformed continuously into each other [23], inducing a kind of connected component structure in loop space. These considerations suggests a possible connection with the logarithm in the complex plane, where the number of times that one winds around the origin could be interpreted as a representation of the solution branch on which one is located. In our case, this winding would be represented by the number of cusps, while the different connected components represent the solution branches. This “duality” will be reported separately.

7. ACKNOWLEDGEMENTS

We would like to thank Igor Cherednikov and Frederik Van der Veken for useful discussions and suggestions.

-
- [1] R. Giles, Phys.Rev. **D24**, 2160 (1981).
 - [2] R. A. Brandt, A. Gocksch, M. Sato, and F. Neri, Phys.Rev. **D26**, 3611 (1982).
 - [3] Y. Makeenko and A. A. Migdal, Phys.Lett. **B88**, 135 (1979).
 - [4] S. Mandelstam, Phys.Rev. **175**, 1580 (1968).
 - [5] L. F. Alday, B. Eden, G. P. Korchemsky, J. Maldacena, and E. Sokatchev, JHEP **1109**, 123 (2011), arXiv:1007.3243 [hep-th].
 - [6] L. F. Alday and J. M. Maldacena, JHEP **0706**, 064 (2007), arXiv:0705.0303 [hep-th].
 - [7] Y. Makeenko and A. A. Migdal, Nucl.Phys. **B188**, 269 (1981).
 - [8] I. O. Cherednikov, T. Mertens, and F. F. Van der Veken, Phys.Rev. **D86**, 085035 (2012), arXiv:1208.1631 [hep-th].
 - [9] J. Munkres, *Analysis on manifolds* Advanced Book Classics (Addison-Wesley Publishing Company, Advanced Book Program, 1991).
 - [10] J. Dieudonne, *Foundations of Modern Analysis* Pure and Applied Mathematics (Read Books, 2008).
 - [11] I. O. Cherednikov, T. Mertens, and P. Taels, In preparation (2013).
 - [12] J. N. Tavares, Int.J.Mod.Phys. **A9**, 4511 (1994), arXiv:9305173 [hep-th].
 - [13] K. T. Chen, Tr. Am. Math. Soc. **89**, 395 (1958).
 - [14] K. T. Chen, J. Alg. **9**, 8 (1968).
 - [15] K. T. Chen, Tr. Am. Math. Soc. **156**, 359 (1971).
 - [16] I. A. Korchemskaya and G. P. Korchemsky, Phys.Lett. **B287**, 169 (1992).
 - [17] A. Bassetto, I. Korchemskaya, G. Korchemsky, and G. Nardelli, Nucl.Phys. **B408**, 62 (1993), arXiv:9303314 [hep-ph].
 - [18] G. P. Korchemsky, J. M. Drummond, and E. Sokatchev, Nucl.Phys. **B795**, 385 (2008), arXiv:0707.0243 [hep-th].
 - [19] Y. Makeenko, Phys.Atom.Nucl. **73**, 878 (2010), arXiv:0906.4487 [hep-th].
 - [20] Y. Makeenko, Acta Phys.Polon. **B39**, 3047 (2008), arXiv:0810.2183 [hep-th].
 - [21] Y. Makeenko, p. 14 (2004), arXiv:0407028 [hep-th].
 - [22] I. Cherednikov, T. Mertens, and P. Taels, In preparation (2013).
 - [23] I. O. Cherednikov, T. Mertens, and P. Taels, In preparation (2013).
 - [24] C. J. Bomhof and P. J. Mulders, Nucl.Phys. **B795**, 409 (2008), arXiv:0709.1390 [hep-ph].
 - [25] I. O. Cherednikov, T. Mertens, P. Taels, and F. F. Van der Veken, (2013), arXiv:1308.3116 [hep-ph].